Original Research

Exenatide protects against hypoxia/reoxygenation-induced apoptosis by improving mitochondrial function in H9c2 cells

Guanglei Chang, Dongying Zhang, Jian Liu, Peng Zhang, Lin Ye, Kai Lu, Qin Duan, Aihua Zheng and Shu Qin

Department of Cardiology, the First Affiliated Hospital of Chongqing Medical University, Chongqing Key Laboratory of Ophthalmology, Chongqing 400016, P. R. China
Corresponding author: Shu Qin. Email: augustlei127@aliyun.com

Abstract

Glucagon-like peptide-1 (GLP-1) analogues might exert the cardioprotective effects via attenuating apoptosis. This study aimed to determine the protective effects and mechanism of exenatide, a GLP-1 analogue, on cardiomyocyte apoptosis using an *in vitro* model of hypoxia/reoxygenation (H/R). H9c2 cells were employed to establish an *in vitro* model of H/R. 200 nM exenatide pretreatment significantly reduced apoptosis measured by flow cytometry. To further study the antiapoptotic mechanism of exenatide, we used flow cytometry in combination with laser confocal microscopy to determine the interaction between exenatide and the process of mitochondria-mediated apoptosis. We found that exenatide pretreatment reduced the intracellular reactive oxygen species (ROS) levels and decreased the mitochondrial calcium overload caused by H/R. Furthermore, an increase of total superoxide dismutase (T-SOD) levels, a decrease of malondialdehyde (MDA) levels, a preservation of mitochondrial membrane potential ($\Delta\Psi m$), a reduction of cytochrome-c release, a decline of cleaved caspase-3 expression, and caspase-3 activation were observed in exenatide-pretreated cultures. These results suggest that exenatide exerts a protective effect on preventing against H/R-induced apoptosis. Importantly, the protective effects of exenatide may be attributed to its role in improving mitochondrial function in H9c2 cells subjected to H/R.

Keywords: GLP-1 analogue, exenatide, hypoxia/reoxygenation, cardiomyocyte apoptosis, mitochondria

***Experimental Biology and Medicine* 2014; 239: 414–422. DOI: 10.1177/1535370214522177**

Introduction

Cardiomyocyte loss due to ischemia/reperfusion (I/R) injury is the major cause of cardiac dysfunction, left ventricular remolding, and heart failure.[1–3] Cell apoptosis induced by I/R is a main type of cardiomyocyte loss, causing a gradual decline of the left ventricular function.[4–6] Many studies have showed that blocking the apoptosis process induced by I/R could reduce cardiomyocyte loss, minimize myocardial injury, and improve ventricular performance.[7] Therefore, the exploration of efficient therapeutic agents inhibiting cardiomyocyte apoptosis in I/R has become a field of interests.[8]

The process of cardiomyocyte apoptosis can be regulated by two main pathways, the extrinsic pathway involving the death receptors[9,10] and the intrinsic pathway depending on mitochondria[9,11,12] and endoplasmic reticulum stress.[13–15] The latter pathway integrates a number of proapoptotic signals in the cardiomyocyte.[9] During reperfusion, the regained oxygen causes a burst of mitochondrial oxidative stress, including a sharply increase of reactive oxygen species (ROS) and reactive nitrogen species (RNS) production.[16,17] The oxidative stress results in a decrease of mitochondrial membrane potential ($\Delta\Psi m$),[18,19] an increase of the mitochondrial calcium overload,[19,20] an induction of the mitochondrial permeability transition pore (mPTP) opening[21,22] and the release of proapoptotic proteins,[23] and subsequently leads to apoptosis.[9] Therefore, protection of mitochondrial function is a promising therapeutic strategy for inhibiting the cardiomyocyte apoptosis in I/R injury.

Exenatide, a glucagon-like peptide-1 (GLP-1) analogue, is a novel drug for the treatment of type 2 diabetes mellitus.[24] The cardioprotective properties of exenatide, especially in I/R injury, have recently been demonstrated in both animal models and in clinical studies.[25,26] Several studies have demonstrated an antiapoptotic effect of GLP-1 on cardiomyocytes.[27–30] However, little is known about the role of exenatide in antiapoptotic effect and the underlying mechanisms in I/R injury. In this study, we used hypoxia/reoxygenation (H/R)-induced apoptosis in H9c2 cells, an established *in vitro* model which resembles I/R

in vivo, in order to investigate whether exenatide protected H9c2 cells from H/R-induced apoptosis by improving mitochondrial function.

Materials and methods

Cell culture and hypoxia/reoxygenation treatment

H9c2 cells (Chinese Academy of Medical Sciences, Shanghai, China) were maintained in Dulbecco's Modified Eagle Media: Nutrient Mixture F-12 (DMEM/F12, Thermo Fisher Biochemical Products, Beijing, China) supplemented with 10% fetal bovine serum (FBS, Invitrogen Life Technologies, Carlsbad, CA, USA) and 100 μg/mL penicillin/streptomycin (Beyotime Institute of Biotechnology, Haimen, China). Hypoxia/reoxygenation (H/R) model was established according to the methods described in previous studies with some modifications.[31] Briefly, when cells were cultured to 70–80% confluence in appropriate culture dishes, they were subjected to hypoxia using DMEM/F12 without FBS and glucose in a hypoxia chamber (Thermo Forma, USA), saturated with a gas mixture (95% N_2 and 5% CO_2) at 37°C. After hypoxia treatment, cells were cultured in the medium with 10% FBS DMEM/F12 in the normal incubating condition. We divided them into four groups: (1) Control group, cells were cultured in the normal incubating condition. (2) Exenatide group, cells were cultured with exenatide (Baxter Pharmaceutical Solutions LLC, Deerfield, IL, USA) in the normal incubating condition. (3) H/R group, cells were subjected to H/R without pretreatment with exenatide. (4) H/R+ exenatide group, cells were pretreated with exenatide for 30 min before subjected to H/R. For flow cytometric analysis, cells were seeded in six-well plates, and for confocal cellular images, cells were seeded onto glass coverslips.

Viability assay

Cell viability was assessed with the cell counting kit-8 (CCK-8, Beyotime Institute of Biotechnology, Haimen, China) as described previously with some modifications.[32] Approximately 1×10^4 H9c2 cells were seeded in 96-well plates for 72 h. Then, cells were pretreated with or without exenatide (0, 50, 100, 200, 400, and 600 nM, respectively) for 30 min before subjected to H/R treatment (4/2, 6/3, 12/4, 14/5, 16/6, 22/10 h). Cells were provided with fresh media and 10 μL of CCK-8 solution was added into every well. Plates were then incubated in the normal incubating condition for 2 h. The optical density values at 470 nm were measured using a microplate reader (Multiskan MK33, Thermolab systems, Helsinki, Finland). Each experiment was repeated for at least three times.

Flow cytometry

Cell apoptosis was detected using flow cytometry.[33] H9c2 cells (2×10^4) were seeded in six-well plates for 72 h. After treatment, cells from four groups were collected, washed twice with cold PBS by centrifugation at 400 *g* for 5 min, and re-suspended at a density of 1×10^6/mL. Cells (500 μL) were mixed with 5 μL Annexin V-fluorescein isothiocyanate and 10 μL propidium iodide (PI, 20 μg/mL) and incubated for 20 min in the dark at room temperature and acquired immediately on flow cytometer. Flow cytometric analysis (Ex. 488 nm/Em. 530 nm) was performed with FACSCalibur cell sorter (BD FACSvantage SE, Beckman Coulter, Brea, CA, USA). The data of fluorescence intensity were analyzed using the cellquest™ software. Each experiment was repeated for at least six times.

In order to quantitative analyze the production of oxidative stress, mitochondrial calcium ($[Ca^{2+}]_m$) and $\Delta\Psi m$, we measured the ROS and RNS generation, $[Ca^{2+}]_m$, $\Delta\Psi m$ using flow cytometry as described previously with some modifications.[33–35] Cells were loaded, respectively, with 2′,7′-dichlorofluorescin diacetate (DCFH-DA, 10 μM, 60 min, Beyotime Institute of Biotechnology, China), dihydroethidium (DHE, 5 μM, 30 min, Beyotime Institute of Biotechnology, Haimen, China), Rhod-2 AM (2 μM, 30 min, Santa Cruz Biotechnology Inc., Santa Cruz, CA, USA), and 5,5′,6,6′-Tetrachloro-1,1′,3,3′-tetraethyl-imidacarbocyanine iodide (JC-1, 10 μg/mL, 20 min, Beyotime Institute of Biotechnology, Haimen, China) at 37°C. The fluorescence intensity was measured using flow cytometry and analyzed using the cellquest™ software. The experiment was repeated at least for three times.

Confocal laser scanning microscope

In order to analyze the production of oxidative stress, we measured the ROS and RNS generation using confocal laser scanning microscope (Leica TCS SP2, Leica Inc., Germany).[33] Cells were loaded with DCFH-DA (10 μM) for 60 min at 37°C and DHE (5 μM) for 30 min at 37°C. DCFH-DA was excited at 488 nm and emitted at 525 nm. DHE was excited at 543 nm and emitted at 560 nm.

The $[Ca^{2+}]_m$ was measured by a mitochondria-permeate calcium fluorophore, Rhod-2 AM (2 μM) for 30 min at 37°C. Rhod-2 AM was excited at 543 nm and emitted at 560 nm.

The fluorescent, lipophilic and cationic probe, JC-1 was employed to measure $\Delta\Psi m$ as described previously.[35] Cells were loaded with JC-1(10 μg/mL) for 20 min at 37°C. Images of the intensities of green (JC-1 monomer) and red (JC-1 aggregate) fluorescence were monitored by emission wavelength at 530 nm and 590 nm. The red fluorescence stands for polarized mitochondria and the green fluorescence stands for depolarized mitochondria in confocal imaging. The confocal images were captured using confocal laser scanning microscope. Each experiment was repeated at least for three times.

Colorimetry

The intracellular total superoxide dismutase (T-SOD) and malondialdehyde (MDA) levels were measured, respectively, using T-SOD assay kit (Jiancheng Bioengineering Institute, Nanjing, China) with 2-(4-Iodophenyl)-3-(4-nitrophenyl)-5 -(2,4-disulfophenyl)-2H-tetrazolium, monosodium salt (2-(4-Iodophenyl)-3-(4-nitrophenyl)-5-(2,4-disulfophenyl)-2H-tetrazolium, monosodium saltWST-1), and lipid peroxidation MDA assay kit (Jiancheng Bioengineering Institute, Nanjing, China) with thiobarbituric acid (TBA) according to the manufacturer's instructions. In brief, cells were seeded in 10 cm culture dish for 72 h.

After indicated treatment, cells were collected and lysed by cell lysis buffer and centrifuged at 1600 *g* for 10 min at 4°C. The supernatants were collected and reacted, respectively, with WST-1 and TBA. Then, the reaction products were measured, respectively, at 450 nm and 532 nm using a spectrophotometer (721D, Pudong Shanghai Physical Optics Instrument Factory, Shanghai, China). The concentrations of T-SOD were expressed as U/mg protein. The concentrations of MDA were expressed as nmol/mg protein. The experiment was repeated at least for three times.

Western blot assay

The cell mitochondria isolation kit (Beyotime Institute of Biotechnology, Haimen, China) was used to fractionate the Cell Mitochondria Isolation Kitcytosol proteins and mitochondria according to the manufacturer's instructions. In brief, cells were seeded in 10 cm culture dish for 72 h. After indicated treatment, cells were collected and homogenated with mitochondria isolation buffer and centrifuged at 600 *g* for 10 min at 4°C. The supernatants were collected and centrifuged at 12,000 *g* for 10 min at 4°C. The supernatants were collected as the cytosol fraction. The protein concentration of cytosol fraction was measured using enhanced BCA protein assay kit (Beyotime Institute of Biotechnology, Haimen, China). Proteins were separated by SDS-PAGE and transferred to membranes. Membranes were blocked in 5% nonfat milk and incubated with primary antibody to cytochrome-c (1:1000, Cell Signaling Technology Inc., Danvers, MA, USA), cleaved caspase-3 (1:1000, Cell Signaling Technology Inc., Danvers, MA, USA), and GAPDH (1:1000, Beyotime Institute of Biotechnology, Haimen, China). Membranes were incubated with secondary antibody. Signals were detected with the ECL system (Beyotime Institute of Biotechnology, Haimen, China). Blots were scanned using Bio-Rad gel imaging system (Bio-Rad, Hercules, CA, USA), and bands were quantified with Quantity One software.

Detection of caspase-3 activity

The caspase-3 activity was measured using caspase-3 activity assay kit (Beyotime Institute of Biotechnology, Haimen, China) according to the manufacturer's instructions. Cells were seeded in 10 cm culture dish for 72 h. After indicated treatment, cells were collected and lysed by cell lysis buffer and centrifuged at 1600 *g* for 20 min at 4°C. The supernatants were collected and reacted, respectively, with acetyl-Asp-Glu-Val-Asp *p*-nitroanilide (Ac-DEVD-pNAAc-DEVD-*p*NA). Then, the reaction products were measured, respectively, at 405 nm using a spectrophotometer (721D, Pudong Shanghai Physical Optics Instrument Factory, Shanghai, China). The experiment was repeated at least for three times. Data were expressed as fold-change in enzyme activity relative to the control group.

Statistical analysis

The SPSS 17.0 software was used for statistical analysis. Data were presented as mean ± standard deviation (SD). Grouped data were analyzed using a one-way analysis of variance (ANOVA) followed by the Student–Newman–Keuls test. When the equal variance test failed, a Mann–Whitney Rank Sum test was used. A P value of less than 0.05 was considered statistically significant.

Results

Exenatide increases the viability of H9c2 cells subjected to H/R

To determine the most reasonable H/R time, cell viability test was performed. After various time of H/R (4/2, 6/3, 12/4, 14/5, 16/6, 22/10 h), H9c2 cell viability was assessed with CCK-8 kit. We found that cell viability was decreased in all the treated groups compared to those in control group (Figure 1(a)). Cell viability after 4/2 h, 6/3 h H/R reduced to 96.58%, 92.24% compared with that in control group ($P < 0.05$), while 12/4, 14/5, 16/6, and 22/10 h H/R reduced cell viability to 70.68%, 60.54%, 53.20%, and

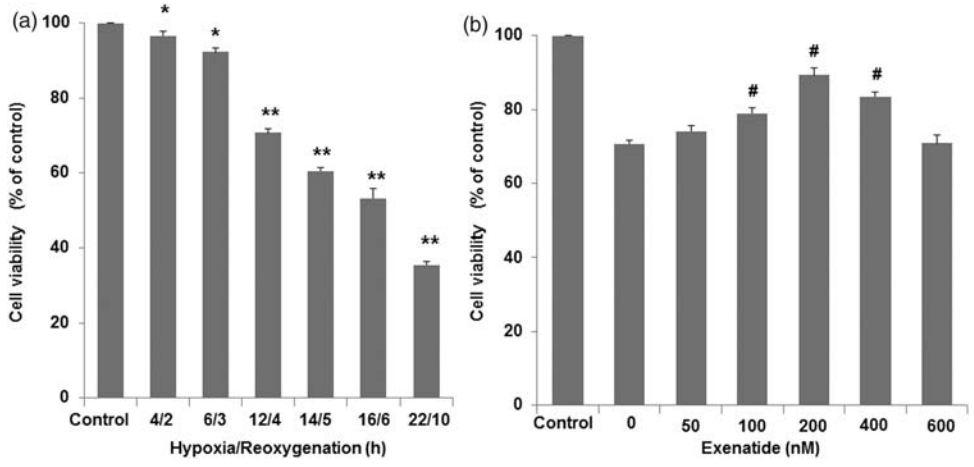

Figure 1 Effects of H/R on the cell viability in H9c2 cells and the protection effects of exenatide in H/R-injury. (a) H9c2 cells were exposed to hypoxia/reoxygenation condition for different time (4/2, 6/3, 12/4, 14/5, 16/6, 22/10 h). (b) H9c2 cells were pretreated with exenatide (0, 50, 100, 200,400, and 600 nM, respectively) for 30 min underwent 12 h hypoxia and then 4 h reoxygenation. After treatment, cell viability was assessed using CCK-8 kit. Data are expressed as percentage of control and represented as mean ± SD, $n = 6$.

*, $P < 0.05$; **, $P < 0.01$ vs. control group. #, $P < 0.05$ vs. the 0 group.

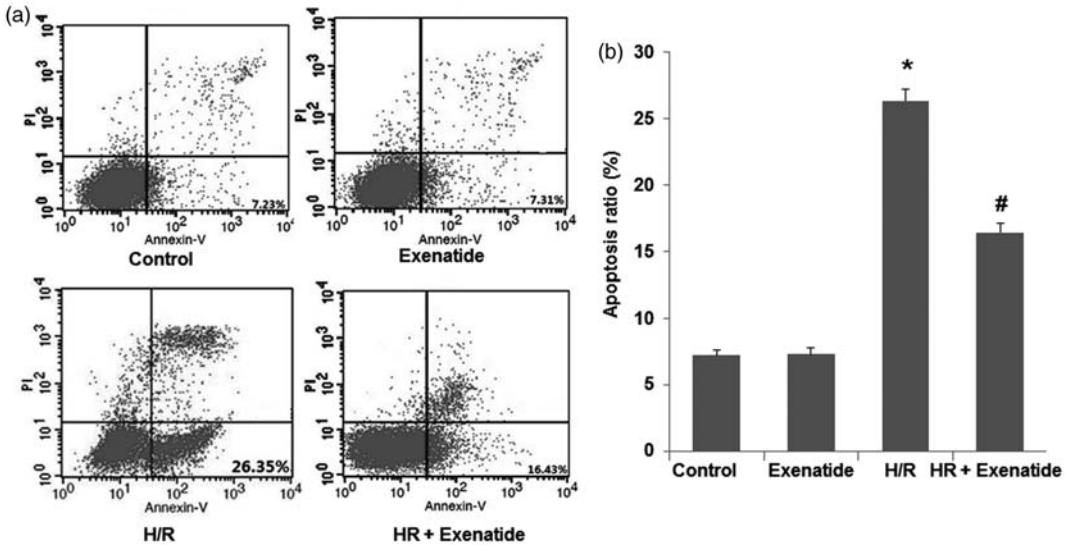

Figure 2 Effects of exenatide on H/R-induced apoptosis in H9c2 cells detected by flow cytometry. H9c2 cells were pretreated with 200 nM exenatide for 30 min prior to H/R treatment. (a) Representative images of flow cytometry. (b) Quantitative analyses of apoptosis ratio by the cellquest^{TM} software. Values are mean ± SD, $n = 3$. *, $P < 0.05$ vs. control group. #, $P < 0.05$ vs. H/R group

35.56% of the control, respectively ($P < 0.01$). We selected 12/4 h H/R to investigate the potential effects of exenatide on cardiomyocyte protection because it is the earliest time point when cell viability showed significant difference ($P < 0.01$).

To examine the possible effects of exenatide on H/R injury, H9c2 cells were pretreated with exenatide (0, 50, 100, 200, 400, and 600 nm, respectively) for 30 min before subjected to H/R treatment. We demonstrated that pretreatment with 100, 200, and 400 nM exenatide could statistically attenuate the loss of cell viability caused by H/R injury ($P < 0.05$) (Figure 1(b)). This result strongly suggested that exenatide did have cardiomyocyte protection ability against the H/R injury in H9c2 cell line. Exenatide, at a concentration of 200 nM, achieved the best efficiency to protect cell viability. Thus, we chose the concentration of 200 nM to treat with cell line in the following experiment.

Exenatide inhibits the H/R-induced apoptosis of H9c2 cells

We investigated the effect of exenatide on the H/R-induced apoptosis in cultured H9c2 cell using flow cytometry. The results of flow cytometry suggested that the apoptotic cells in H/R treatment group were higher than those in control group ($P < 0.05$, Figure 2). Pretreatment with 200 nM exenatide decreased the amount of apoptotic cells in comparison to the H/R group ($P < 0.05$), suggesting that exenatide could inhibit the H/R-induced apoptosis of H9c2 cells.

Exenatide reduces the H/R-induced oxidative stress in H9c2 cells

It is known that increased oxidative stress can positively regulate apoptosis, thus we examined the effect of exenatide on the H/R-induced oxidative stress in H9c2 cells. The production of ROS and RNS was measured using flow cytometry and confocal laser scanning microscope (Figure 3). In the H/R group, the production of ROS (green) and RNS (red) in the mitochondria was significantly increased, and exenatide pretreatment suppress their production (Figure 3(a) and (c)). Quantitative data from flow cytometry agreed with qualitative findings from confocal imaging (Figure 3(b) and (d)). We found that the production of ROS and RNS was significantly elevated in the H/R group compared with those of the control group ($P < 0.05$). However, pretreatment with 200 nM exenatide significantly decreased the H/R-induced ROS and RNS generation ($P < 0.05$).

To determine the antioxidative effects of exenatide on H/R injury, we further measured the intracellular levels of T-SOD (a key antioxidant enzyme) and MDA (one product of oxidative stress) in all groups (Figure 4(a) and (b)). MDA level was significantly increased in H/R group compared with control group, while T-SOD level was decreased ($P < 0.05$). When compared with H/R group, pretreatment with exenatide 200 nM decreased significantly MDA level and increased T-SOD level ($P < 0.05$), suggesting the antioxidative effects of exenatide.

Exenatide reduces the H/R-induced mitochondrial calcium overload in H9c2 cells

Due to the known effect of oxidative stress on Ca^{2+}, we tested the mitochondrial Ca^{2+} ($[Ca^{2+}]_m$) using flow cytometry and confocal laser scanning microscope (Figure 5). Unsurprisingly, H/R treatment enhanced the $[Ca^{2+}]_m$ in the mitochondria compared with that of in control group, while pretreatment with 200 nM exenatide showed opposite effect (Figure 5(a)). Meanwhile, quantitative analysis of flow cytometry was in consistent with previous results ($P < 0.05$) (Figure 5(b)).

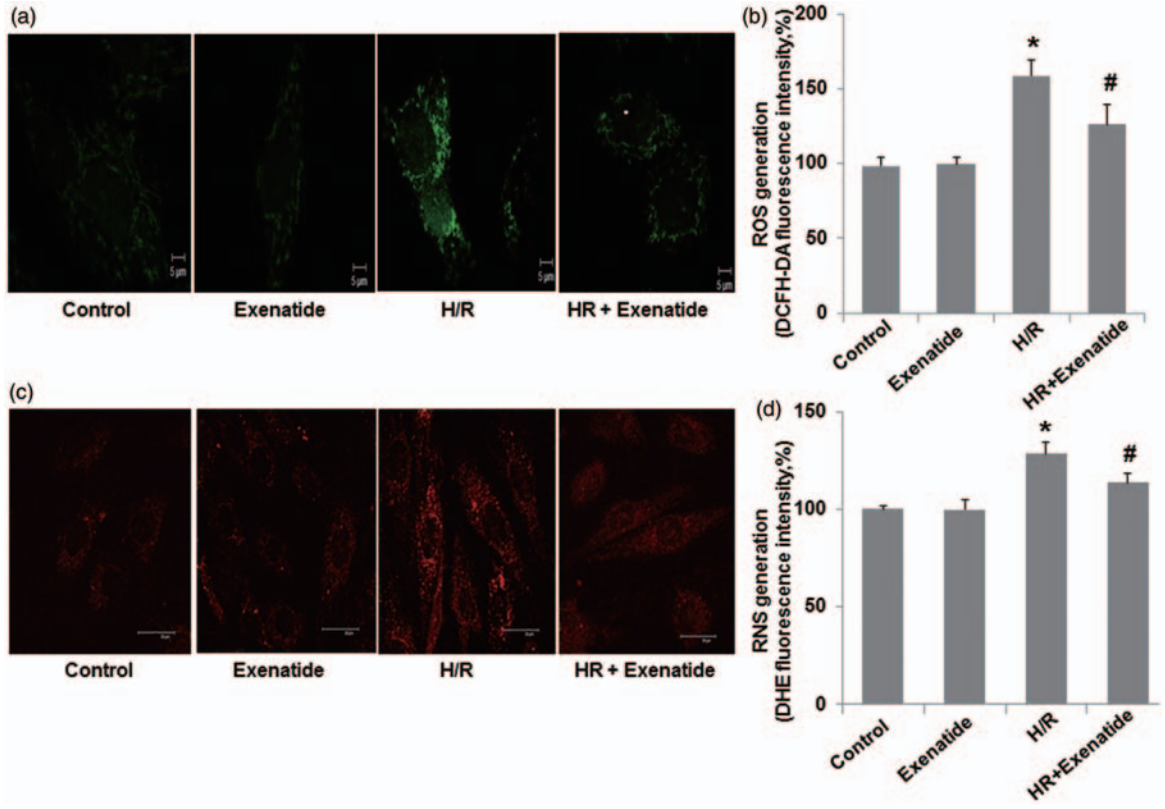

Figure 3 Effects of exenatide on ROS and RNS generation in H9c2 cells. Pretreated with 200 nM exenatide for 30 min, cells were subjected to H/R. The treated cells were detected by confocal microscopy and flow cytometry. (a) ROS generation was estimated using the probe DCFH-DA (green fluorescence) by confocal microscopy. Scale bar: 5 μm. Images presented are representative of three independent experiments. (b) Quantitative analyses of DCFH-DA fluorescence intensity using flow cytometry. Values are mean ± SD, $n = 3$. *, $P < 0.05$ vs. control group. #, $P < 0.05$ vs. H/R group. (c) RNS generation was estimated using the probe DHE (red fluorescence) by confocal microscopy. Scale bar: 5 μm. Images presented are representative of three independent experiments. (d) Quantitative analyses of DHE fluorescence intensity using flow cytometry. Values are mean ± SD, $n = 3$. *, $P < 0.05$ vs. control group. #, $P < 0.05$ vs. H/R group. (A color version of this figure is available in the online journal.)

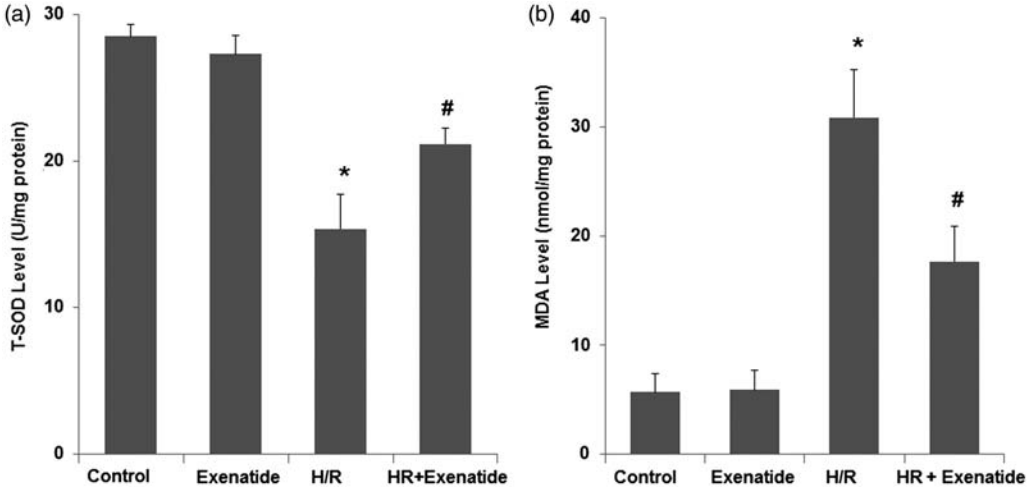

Figure 4 Effects of exenatide on T-SOD and MDA levels in H9c2 cells. (a) Cellular T-SOD levels were measured using the WST method, and the concentrations of T-SOD were expressed as U/mg protein. (b) Cellular MDA levels were measured using the TBA method, and the concentrations of MDA were expressed as nmol/mg protein. Values are mean ± SD, $n = 6$. *, $P < 0.05$ vs. control group. #, $P < 0.05$ vs. H/R group

Exenatide inhibits the mitochondrial apoptotic pathway

Opening of mPTP can lead to the release of proapoptotic molecules, which initiate apoptosis via caspas-3 dependent pathway. We observed the cytochrome-c release and cleaved caspase-3 expression in H9c2 cells using Western blot. The cytochrome-c release and cleaved caspase-3 expression were significantly enhanced in H/R group compared with those in the control group ($P < 0.05$, Figure 6(a)

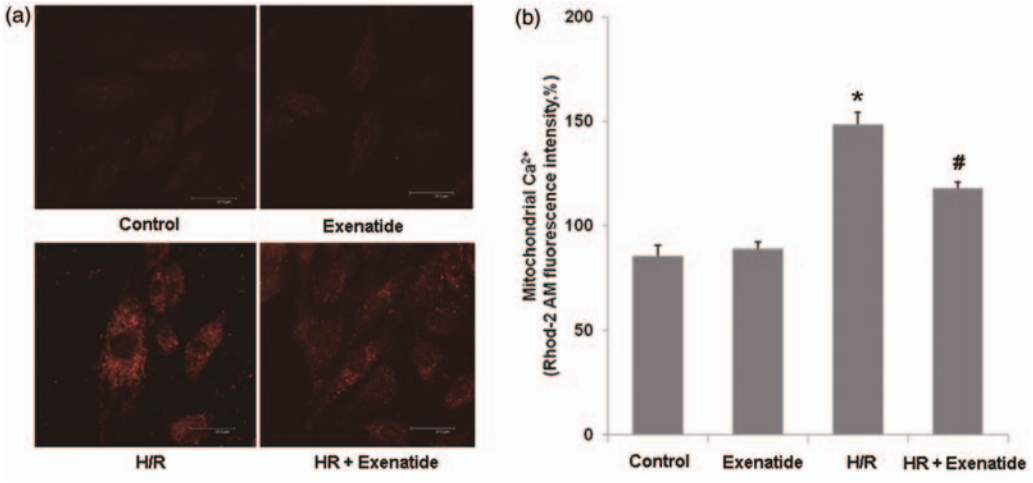

Figure 5 Effects of exenatide on mitochondrial calcium in H9c2 cells. Pretreated with 200 nM exenatide for 30 min, cells were subjected to H/R. The treated cells were detected by confocal microscopy and flow cytometry. (a) Mitochondrial calcium was estimated using the probe Rhod-2 AM (red fluorescence) by confocal microscopy. Scale bar: 37.5 μm. Images presented are representative of three independent experiments. (b) Quantitative analyses of Rhod-2 AM fluorescence intensity using flow cytometry. Values are mean ± SD, $n = 3$. *, $P < 0.05$ vs. control group. #, $P < 0.05$ vs. H/R group. (A color version of this figure is available in the online journal.)

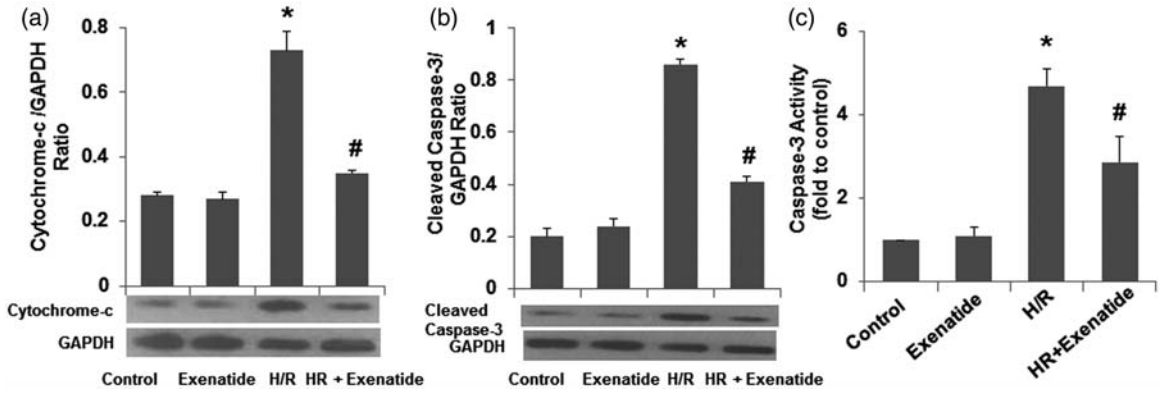

Figure 6 Effects of exenatide on cytochrome-c release, cleaved caspase-3 expression, and caspase-3 activity in H9c2 cells. (a) The cytochrome-c release was measured by Western blot, and data were expressed as ratio of cytochrome-c to GAPDH. (b) The cleaved caspase-3 expression was measured by Western blot, and data were expressed as ratio of cleaved caspase-3 to GAPDH. (c) The caspase-3 activity was measured using the caspase-3 activity assay kit, and data were expressed as fold-change from the control group. Values are mean ± SD, $n = 6$. *, $P < 0.05$ vs. control group. #, $P < 0.05$ vs. H/R group

and (b)), while both were markedly reduced by 200 nM exenatide pretreatment ($P < 0.05$).

We further investigated the effect of exenatide on the caspase-3 activation using the caspase-3 activity assay kit (Figure 6(c)). We found that the caspase-3 activity in H/R group was higher than that of the control group ($P < 0.05$), and exenatide pretreatment significantly reduced the caspase-3 activity compared with that of H/R group ($P < 0.05$). Our results suggested that exenatide can repress the activation of caspase-3 expression and its activity induced by H/R.

Exenatide prevents the H/R-induced the depolarization of mitochondrial potential in H9c2 cells

To further investigate the effects of exenatide on the mitochondrial function, the ΔΨm was determined using JC-1 probe by flow cytometry and confocal laser scanning microscope (Figure 7). The JC-1 probe was detected in both polarized (red) and depolarized (green) mitochondria in confocal imaging (Figure 7(a)). Cells subjected to H/R showed a decrease in polarized mitochondria and an increase in depolarized mitochondria, and exenatide pretreatment reversed the changes in fluorescence signal. The fluorescence ratio of red to green ΔΨm was quantitated by flow cytometry (Figure 7(b)), thus a low ratio suggested mitochondrial depolarization. ΔΨm was lower in H/R group than in control group ($P < 0.05$), and exenatide pretreatment significantly increased the ratio compared with that of H/R group ($P < 0.05$). These findings suggested that exenatide prevented the ΔΨ depolarization in H/R.

Discussion

In this study, we investigated the effects of exenatide on cardiomyocyte apoptosis and mitochondrial dysfunction

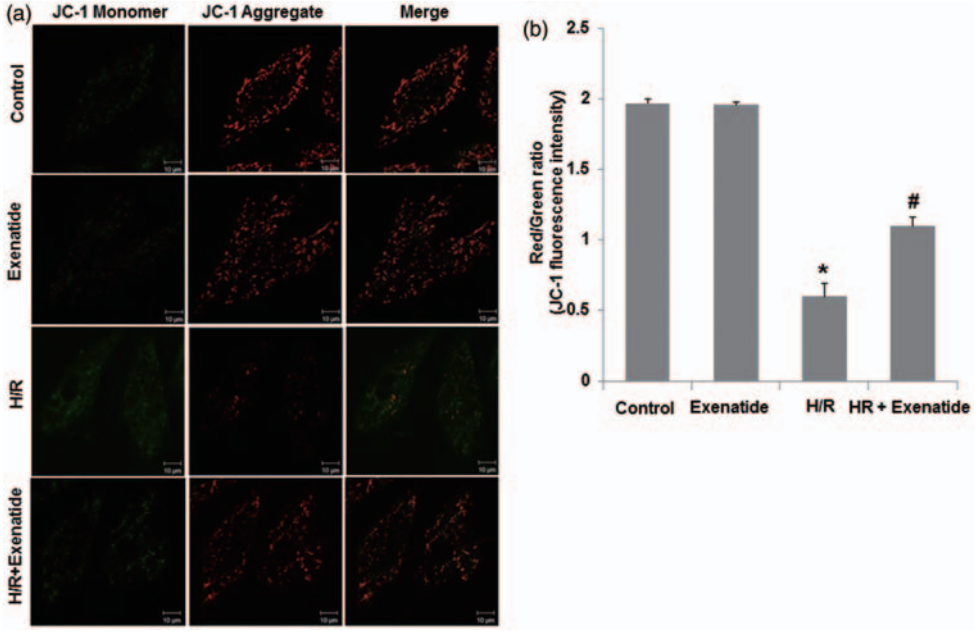

Figure 7 Effects of exenatide on mitochondrial membrane potential in H9c2 cells.
Pretreated with exenatide (200 nM) for 30 min, cells were subjected to H/R. The treated cells were detected by confocal microscopy and flow cytometry. (a) The probe JC-1 was employed to measure $\Delta\Psi m$ by confocal microscopy. Red fluorescence is from JC-1 aggregate in mitochondria with polarized inner mitochondrial membranes, while green fluorescence is from JC-1 monomer and indicates $\Delta\Psi m$ depolarization. Images presented are representative of three independent experiments. Scale bar: 10 μm. (b) The fluorescence ratio of red to green was quantitated by flow cytometry. Values are mean ± SD, $n = 3$. *, $P < 0.05$ vs. control group. #, $P < 0.05$ vs. H/R group. (A color version of this figure is available in the online journal.)

in H9c2 cells subjected to H/R injury. We found that pretreatment of exenatide provided H9c2 cells a strong protection from H/R-induced apoptosis by improving the mitochondrial function through reducing mitochondrial oxidative stress, attenuating mitochondrial Ca^{2+} accumulation, preserving $\Delta\Psi m$, and so on. This study firstly assesses and demonstrates a relation between the antiapoptotic actions of exenatide and mitochondrial function in H9c2 cells in response to the H/R injury.

I/R-induced cardiomyocyte apoptosis has been confirmed as a causative factor in the development of cardiac dysfunction, and mitochondrial dysfunction has been shown to participate in the induction of apoptosis.[7,9] This study showed that apoptosis is important in H/R injury, and H/R-induced apoptosis is closely associated with mitochondrial dysfunction. Importantly, the pretreatment of exenatide significantly inhibits the H/R-induced apoptosis in H9c2 cells. The antiapoptotic effects of GLP-1 on the cardiomyocytes via extrinsic pathway have been examined in previous studies,[27–30] while our study focused on the mitochondria-dependent pathway.

Mitochondria not only provide energy for cardiomyocytes but also play vital role in cardiomyocyte apoptotic signaling pathway.[12] Mitochondria dysfunction is a predominant cause of H/R-induced cardiomyocyte apoptosis.[11,35] This study showed the protective role of exenatide in mitochondria via reducing mitochondrial oxidative stress, attenuating mitochondrial Ca^{2+} accumulation, and preserving $\Delta\Psi m$ under the H/R condition.

Mitochondria are the major sources of oxidative stress and play a crucial role in oxidative injury during H/R.[36] Mitochondrial malfunction can induce the production of oxidative stress and reduce the adenosine triphosphate synthesis. ROS and RNS are products of mitochondrial oxidative stress. Generation of ROS is an important step in the mitochondria-dependent apoptosis pathway induced by H/R.[37,38] Consistent with previous studies, the levels of ROS and RNS increased in the H/R treatment H9c2 cells.[31,35] Our results further demonstrated that H/R-induced ROS and RNS generations were efficiently attenuated by exenatide. In addition, we further measured the intracellular levels of T-SOD (a key antioxidant enzyme) and MDA (one product of oxidative stress) in all groups to determine the antioxidative action of exenatide on H/R injury. We found that T-SOD levels decreased and MDA levels increased in H/R-treated H9c2 cells, while exenatide treatment increased T-SOD levels and decreased MDA levels under the H/R condition. The mitochondrial respiratory chain at complexes I and III have long been considered as the center site of ROS production.[39] Moreover, the endogenous free scavengers such as SOD could suppress ROS levels.[40] On the basis of others and our data,[39,40] we hypothesize that antioxidative effects of exenatide should be accounted for its ability to protect respiratory chain or improvement of the endogenous antioxidant reserve.

Previous studies have reported that the mitochondrial ROS production might be associated with the disruption of mitochondrial Ca^{2+} homeostasis.[16,20,41] In this study, we demonstrated that not only ROS production but also

the influx of Ca^{2+} into mitochondria during H/R was significantly induced. Importantly, we observed a significant decrease of mitochondrial Ca^{2+} accumulation in exenatide treated cells. Therefore, we suspected that exenatide might reduce the H/R-induced ROS production by inhibiting the mitochondrial Ca^{2+} overload.

mPTP is a nonspecific pore in the inner mitochondrial membrane, which is permeable to small molecules. Opening of mPTP is a key mechanism of mitochondrial injury under I/R conditions.[16,42] ROS generation and mitochondrial Ca^{2+}accumulation are key inducers of mPTP opening. Moreover, the opening of mPTP can lead to the collapse of $\Delta\Psi m$ and the release of proapoptotic molecules including cytochrome-c and apoptotic peptidase activating factor-1(Apaf-1).[43] After exenatide treatment, H/R-induced $\Delta\Psi m$ depolarization was significantly alleviated, and the release of cytochrome-c from mitochondrial matrix into cytosol was effectively inhibited. After the cytochrome-c releases into the cytosol, apotosomes are formed and subsequently activate the procaspase-9, which in turn amplifies the downstream caspases such as caspase-3 to initiate apoptosis.[44] Here, we demonstrated that exenatide pretreatment suppressed the caspase-3 expression and activity in H/R-treated H9c2 cells. Recent studies have revealed that GLP-1 receptor agonist Exendin-4 participates in the intrinsic apoptosis process by inhibiting the mitochondrial pathway.[45] Although the underlying mechanisms required further work, our data clearly showed that exenatide preserves the mitochondrial function and inhibits the mitochondria-dependent pathway.

In conclusion, we document protective effects of exenatide against H/R-induced apoptosis in H9c2 cells via improving mitochondrial function. Interactions between exenatide and mitochondria provided a new strategy to prevent the H/R-induced apoptosis by attenuating the intrinsic apoptotic pathway. Of course, more intensive studies *in vivo* are required to evaluate the cardioprotective effects of exenatide, and the exact molecular mechanism will be clarified.

Author contributions: All authors participated in the design, interpretation of the studies and analysis of the data; GC, DZ, JL, and SQ conceived the experiments, GC, PZ, LY, and KL performed the experiments, GC and SQ wrote the manuscript, and GC, DZ, JL, QD, and AZ carried out review of the manuscript.

ACKNOWLEDGMENTS

This work was supported by the National Natural Science Fund (Grant no. 81100196), Natural Science Foundation Project of CQ CSTC (Grant no. CSTC, 2011BB5133), Foundation project of Traditional Chinese Medicine of Chongqing Municipal Health Bureau (Grant no. 2012-2-125), and Pfizer pharmaceutical limited competition grants (Grant no. ws1790576). We greatly appreciate Jianyong Wu, Dezhang Zhao, and Xiaoyun Dou (Institute of Life Sciences, Chongqing Medical University) for excellent technical support for the flow cytometry analysis and confocal microscopy.

REFERENCES

1. Pfeffer MA, Braunwald E. Ventricular remodeling after myocardial infarction. Experimental observations and clinical implications. *Circulation* 1990;**81**:1161–72
2. Anversa P, Cheng W, Liu Y, Leri A, Redaell G, Kajstura J. Apoptosis and myocardial infarction. *Basic Res Cardiol* 1998;**93**:8–12
3. Palojoki E, Saraste A, Eriksson A, Pulkki K, Kallajoki M, Voipio-Pulkki LM, Tikkanen I. Cardiomyocyte apoptosis and ventricular remodeling after myocardial infarction in rats. *Am J Physiol Heart Circ Physiol* 2001;**280**:H2726–31
4. Kajstura J, Cheng W, Reiss K, Clark WA, Sonnenblick EH, Krajewski S, Reed JC, Olivetti G, Anversa P. Apoptotic and necrotic myocyte cell deaths are independent contributing variables of infarct size in rats. *Lab Invest* 1996;**4**:86–107
5. Saraste A, Pulkki K, Kallajoki M, Henriksen K, Parvinen M, Voipio-Pulkki LM. Apoptosis in human acute myocardial infarction. *Circulation* 1997;**95**:320–3
6. Regula KM, Kirshenbaum LA. Apoptosis of ventricular myocytes: a means to an end. *J Mol Cell Cardiol* 2005;**38**:3–13
7. Lee Y, Gustafsson AB. Role of apoptosis in cardiovascular disease. *Apoptosis* 2009;**14**:536–48
8. Favaloro B, Allocati N, Graziano V, Di Ilio C, De Laurenzi V. Role of apoptosis in disease. *Aging (Albany NY)* 2012;**4**:330–49
9. Crow MT, Mani K, Nam YJ, Kitsis RN. The mitochondrial death pathway and cardiac myocyte apoptosis. *Circ Res* 2004;**95**:957–70
10. Danial NN, Korsmeyer SJ. Cell death: critical control points. *Cell* 2004;**116**:205–19
11. Sarkey JP, Chu M, McShane M, Bovo E, Mou YA, Zima AV, de Tombe PP, Kartje GL, Martin JL. Nogo-A knockdown inhibits hypoxia/reoxygenation-induced activation of mitochondrial-dependent apoptosis in cardiomyocytes. *J Mol Cell Cardiol* 2011;**50**:1044–55
12. Li Q, Zhou LY, Gao GF, Jiao JQ, Li PF. Mitochondrial network in the heart. *Protein Cell* 2012;**3**:410–8
13. Azfer A, Niu J, Rogers LM, Adamski FM, Kolattukudy PE. Activation of endoplasmic reticulum stress response during the development of ischemic heart disease. *Am J Physiol Heart Circ Physiol* 2006;**291**:H1411–20
14. Minamino T, Kitakaze M. ER stress in cardiovascular disease. *J Mol Cell Cardiol* 2010;**48**:1105–10
15. Gorman AM, Healy SJ, Jäger R, Samali A. Stress management at the ER: regulators of ER stress-induced apoptosis. *Pharmacol Ther* 2012;**134**:306–16
16. Honda HM, Korge P, Weiss JN. Mitochondria and ischemia/reperfusion injury. *Ann N Y Acad Sci* 2005;**1047**:248–58
17. Chen Q, Moghaddas S, Hoppel CL, Lesnefsky EJ. Ischemic defects in the electron transport chain increase the production of reactive oxygen species from isolated rat heart mitochondria. *Am J Physiol Cell Physiol* 2008;**294**:C460–6
18. Zamzami N, Marchetti P, Castedo M, Hirsch T, Susin SA, Masse B, Kroemer G. Inhibitors of permeability transition interfere with the disruption of the mitochondrial transmembranepotential during apoptosis. *FEBS Lett* 1996;**384**:53–7
19. Ylitalo KV, Ala-Rämi A, Liimatta EV, Peuhkurinen KJ, Hassinen IE. Intracellular free calcium and mitochondrial membrane potential in ischemia/reperfusion and preconditioning. *J Mol Cell Cardiol* 2000;**32**:1223–38
20. Shintani-Ishida K, Inui M, Yoshida K. Ischemia-reperfusion induces myocardial infarction through mitochondrial Ca^{2+} overload. *J Mol Cell Cardiol* 2012;**53**:233–9
21. Hausenloy DJ, Yellon DM, Mani-Babu S, Duchen MR. Preconditioning protects by inhibiting the mitochondrial permeability transition. *Am J Physiol Heart Circ Physiol* 2004;**287**:H841–9
22. Hoshovs'ka IuV, Shymans'ka TV, Rudyk OV, Korkach IuP, Sahach VF. Mitochondria permeability transition as a target for ischemic preconditioning. *Fiziol Zh* 2011;**57**:34–45
23. Lundberg KC, Szweda LI. Preconditioning prevents loss in mitochondrial function and release of cytochrome c during prolonged cardiac ischemia/reperfusion. *Arch Biochem Biophys* 2006;**453**:130–4

24. Garber AJ. Novel GLP-1 receptor agonists for diabetes. *Expert Opin Investig Drugs* 2012;**21**:45–57
25. Timmers L, Henriques JP, de Kleijn DP, Devries JH, Kemperman H, Steendijk P, Verlaan CW, Kerver M, Piek JJ, Doevendans PA, Pasterkamp G, Hoefer IE. Exenatide reduces infarct size and improves cardiac function in a porcine model of ischemia and reperfusion injury. *J Am Coll Cardiol* 2009;**53**:501–10
26. Chiquette E, Toth PP, Ramirez G, Cobble M, Chilton R. Treatment with exenatide once weekly or twice daily for 30 weeks is associated with changes in several cardiovascular risk markers. *Vasc Health Risk Manag* 2012;**8**:621–9
27. Xie Y, Wang SX, Sha WW, Zhou X, Wang WL, Han LP, Li DQ, Yu DM. Effects and mechanism of glucagon-like peptide-1 on injury of rats cardiomyocytes induced by hypoxia-reoxygenation. *Chin Med J (Engl)* 2008;**121**:2134–8
28. Ravassa S, Zudaire A, Carr RD, Díez J. Antiapoptotic effects of GLP-1 in murine HL-1 cardiomyocytes. *Am J Physiol Heart Circ Physiol* 2011;**300**:H1361–72
29. Ravassa S, Zudaire A, Díez J. Glucagon-like peptide 1 and cardiac cell survival. *Endocrinol Nutr* 2012;**59**:561–9
30. Wright EJ, Farrell KA, Malik N, Kassem M, Lewis AL, Wallrapp C, Holt CM. Encapsulated glucagon-like peptide-1-producing mesenchymal stem cells have a beneficial effect on failing pig hearts. *Stem Cells Transl Med* 2012;**1**:759–69
31. Park M, Youn B, Zheng XL, Wu D, Xu A, Sweeney G. Globular adiponectin, acting via AdipoR1/APPL1, protects H9c2 cells from hypoxia/reoxygenation-induced apoptosis. *PloS One* 2011;**6**:e19143
32. Wang L, Wang ZH, Shen CY, You ML, Xiao JF, Chen GQ. Differentiation of human bone marrow mesenchymal stem cells grown in terpolyesters of 3-hydroxyalkanoates scaffolds into nerve cells. *Biomaterials* 2010;**31**:1691–8
33. Kumar S, Kain V, Sitasawad SL. High glucose-induced Ca^{2+} overload and oxidative stress contribute to apoptosis of cardiac cells through mitochondrial dependent and independent pathways. *Biochim Biophys Acta* 2012;**1820**:907–20
34. Odagiri K, Katoh H, Kawashima H, Tanaka T, Ohtani H, Saotome M, Urushida T, Satoh H, Hayashi H. Local control of mitochondrial membrane potential, permeability transition pore and reactive oxygen species by calcium and calmodulin in rat ventricular myocytes. *J Mol Cell Cardiol* 2009;**46**:989–97
35. Yue R, Hu H, Yiu KH, Luo T, Zhou Z, Xu L, Zhang S, Li K, Yu Z. Lycopene protects against hypoxia/reoxygenation – induced apoptosis by preventing mitochondrial dysfunction in primary neonatal mouse cardiomyocytes. *PloS One* 2012;**7**:e50778
36. Poyton RO, Ball KA, Castello PR. Mitochondrial generation of free radicals and hypoxic signaling. *Trends Endocrinol Metab* 2009;**20**:332–40
37. Becker LB, vandenHoek TL, Shao ZH, Li CQ, Schumacker PT. Generation of superoxide in cardiomyocytes during ischemia before reperfusion. *Am J Physiol* 1999;**277**:H2240–6
38. Becker LB. New concepts in reactive oxygen species and cardiovascular reperfusion physiology. *Cardiovasc Res* 2004;**61**:461–70
39. Chen Q, Vazquez EJ, Moghaddas S, Hoppel CL, Lesnefsky EJ. Production of reactive oxygen species by mitochondria. *J Biol Chem* 2003;**278**:36027–31
40. Cortassa S, Aon MA, Winslow RL, O'Rourke B. A mitochondrial oscillator dependent on reactive oxygen species. *Biophys J* 2004;**87**:2060–73
41. Ott M, Gogvadze V, Orrenius S, Zhivotovsky B. Mitochondria, oxidative stress and cell death. *Apoptosis* 2007;**12**:913–22
42. Weiss JN, Korge P, Honda HM, Ping P. Role of the mitochondrial permeability transition in myocardial disease. *Circ Res* 2003;**93**:292–301
43. Patterson SD, Spahr CS, Daugas E, Susin SA, Irinopoulou T, Koehler C, Kroemer G. Mass spectrometric identification of proteins released from mitochondria undergoing permeability transition. *Cell Death Differ* 2000;**7**:137–44
44. Galluzzi L, Morselli E, Kepp O, Kroemer G. Targeting post mitochondrial effectors of apoptosis for neuroprotection. *Biochim Biophys Acta* 2009;**1787**:402–13
45. Wei Q, Sun YQ, Zhang J. Exendin-4, a glucagon-like peptide-1 receptor agonist, inhibits cell apoptosis induced by lipotoxicity in pancreatic β-cell line. *Peptides* 2012;**37**:18–24

(Received June 27, 2013, Accepted December 6, 2013)